As a circuit element a ring resonator of this kind has the property that no wave is reflected back to the source. It is matched at any frequency. Besides this no wave is transmitted at the critical coupling. In this special case all the power is consumed in the ring giving an ideal absorption filter for the resonance frequency [12]. Two or more ring resonators can be placed one after the other to obtain a filter of arbitrary absorption curve. The resulting transmission coefficient is simply the product of the individual transmission coefficient.

At a wavelength of 4 mm the measured loaded Q of the TEM_{00q}-mode at low coupling was 200 000. The theoretical unloaded Q is 250 000 using the dc conductivity of Al and neglecting diffraction losses. At a wavelength of 1.8 cm the corresponding values for the larger ring resonator are: measured loaded $Q=130\,000$ and theoretical $Q_0=200\,000$.

An interesting property of a ring resonator is its degeneracy with respect to the propagation direction of the wave. The wave can circulate clockwise and counterclockwise. Normally only one wave is excited, but if a coupling of the two waves is introduced by placing a dielectric sheet or something else in the path as shown in Fig. 5, standing waves are excited, the resonance splits up, and two resonance frequencies appear (Fig. 6). These two frequencies correspond to different standing wave patterns. In one case the dielectric sheet lies in the plane of a maximum of the electric field (lower frequency), in the other case it lies in a minimum of the electric field (higher frequency).[1] The splitting is a function of the reflection coefficient r of the sheet. The theory gives the relative distance of the two resonance frequencies as

$$\frac{\Delta\omega}{\omega} = \frac{\lambda}{\pi L} \cdot \arctan \sqrt{\frac{r^2 - (\pi L/\lambda Q)^2}{[1 - r^2][1 + (\pi L/\lambda Q)^2]}}, \quad \frac{\pi L}{\lambda Q} \ll 1, \; r \geq \frac{\pi L}{\lambda Q}. \quad (2)$$

r = reflection coefficient of the coupling element (sheet),
λ = wavelength,
L = perimeter of the triangle = length of the optical round path,
Q = loaded quality factor of the resonator without the coupling element.

Only if the Q of the resonance is sufficiently high can the two resonances be resolved. This is the case if $r > \pi L/\lambda Q$. At small reflection coefficient and $r \gg \pi L/\lambda Q$ (2) reduces to

$$\frac{\Delta\omega}{\omega} \approx \frac{\lambda r}{\pi L}.$$

The reflection coefficient is transformed directly into the frequency scale and thus can be measured with high precision. By this method permittivities of thin dielectric foils have been measured at 17 GHz (Fig. 6). The smallest r which could be measured is

$$r \approx 0.001$$

[1] The phenomenon may be illustrated by the well-known coupled pendula. Without coupling each pendulum represents one of the two degenerate circulating waves in resonance. If coupled by a spring or the like, the system of the pendula shows two frequencies which are separated by the beat frequency.

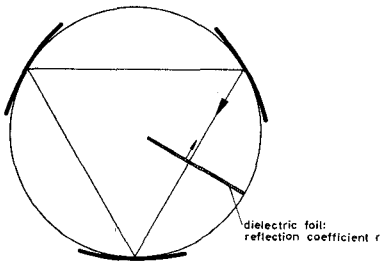

Fig. 5. Coupling of the two degenerate modes by a dielectric sheet with a reflection coefficient r.

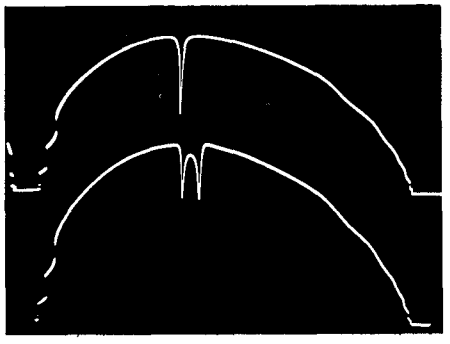

Fig. 6. Transmitted power vs. frequency of the 17 GHz ring resonator. The upper trace shows the resonance curve of the TEM_{00q}-mode. The lower trace shows the effect of a dielectric foil (0.03 mm thick) when placed in the resonator as shown in Fig. 5. The distance of the two resonances is 1.7 MHz.

for the 17 GHz as well as for the 70 GHz band.

Conclusion

Quasi-optical ring resonators for microwaves, millimeterwaves, and submillimeterwaves have interesting properties as circuit elements and measuring instruments. The fact that a ring resonator is always matched and that total absorption at the resonance frequencies is possible, makes it especially suitable for filtering and controlling purposes. Coupling of the two degenerate modes allows the measurement of small reflection cofficients not attainable with conventional methods.

The splitting of the two resonant modes may find an important application in laser technology: a ring laser may be constructed which radiates at two frequencies with a frequency difference adjustable from zero to $c/2L$ [see (2)]. For laser mixing experiments this means that the beat frequency can be varied continuously by introducing a variable coupling.

G. Schulten
Philips Zentrallaboratorium
GmBH
Hamburg-Stellingen
Germany

References

[1] W. M. Macek and D. T. M. Davis, "Rotation rate sensing with traveling-wave ring lasers, *Appl. Phys. Lett.*, vol. 2, p. 67, February 1963.
[2] W. M. Macek, J. R. Schneider, and R. M. Salamon, "Measurement of Fresnel drag with ring laser," *J. Appl. Phys.*, vol. 35, p. 2556, August 1964.
[3] P. O. Clark, "Multireflector optical resonators," *Proc. IEEE*, vol. 51, p. 949, June 1963.
[4] S. A. Collins, Jr., "Analysis of optical resonators involving focussing elements," *Appl. Opt.*, vol. 3, p. 1263–1275, November 1964.
[5] S. A. Collins, Jr., and D. T. M. Davis, "Modes in a triangular ring optical resonator," *Appl. Opt.*, vol. 3, p. 1314–1315, November 1964.
[6] W. W. Rigrod, "The optical ring resonator," *Bell Sys. Tech. J.*, vol. 44, p. 9, May–June 1965.
[7] F. J. Tischer, "Resonance properties of ring circuits," *IRE Trans. on Microwave Theory and Techniques*, vol. MTT-5, p. 51, January 1957.
[8] J. E. Degenford, M. D. Sirkis, and W. H. Steier, "The reflecting beam waveguide," *IEEE Trans. on Microwave Theory and Techniques*, vol. MTT-12, p. 445, July 1964.
[9] G. D. Boyd and J. P. Gordon, "Confocal multimode resonator for mm through optical wavelength masers," *Bell Sys. Tech. J.*, vol. 40, p. 489, 1961.
[10] G. Schulten, "Quasioptische Resonatoren mit mehr als zwei Spiegeln," Philips Zentrallaboratorium GmBH, Hamburg, Laborbericht 76, November 1965.
[11] J. A. Stratton, *Electromagnetic Theory*. New York: McGraw-Hill, 1941, ch. IX.
[12] G. Schulten, "Resonatoren für Millimeterwellen und ihre Verwendung zur Beobachtung von Gasresonanzen," *Frequenz*, vol. 20, p. 10, January 1966.

Cross Polarization in a General Two Plate Polarizer

A common type of polarizer consists of two quarter-wave plates in a circular TE_{11} mode waveguide. Ideally, the first plate converts linear to circular polarization, and the second rotatable plate converts from circular to linear polarization at an angle $\pi/4$ to this plate. The plates take various forms such as dielectric vanes[1] and disks,[2] or capacitive pins.[3]

This ideal situation does not exist over a finite bandwidth, and perhaps not even at any given frequency; and a cross-polarized output component is present. Values of this cross-polarization for arbitrary vane angles and differential phase shifts would be useful in predicting the performance over a bandwidth of a polarizer using elements of known frequency vs. differential phase shift characteristics.

This correspondence contains generalized curves for the worst cross polarization with rotation for arbitrary values of angular setting of the first vane ϕ_1, and differential phase shifts of θ_1, θ_2 for the first and second vanes, respectively, as shown in Fig. 1. The analysis assumes lossless elements throughout.

Assuming that $E_i = \cos \omega t$ in the direction shown, one finds the output components of E parallel and perpendicular to plate 2 (E_{21}, E_{22}, respectively) to be

$$\begin{aligned} E_{21} &= \cos(T - \theta_1 - \theta_2)\cos\phi_1\cos(\phi_1 - \phi_2) \\ &\quad + \cos(T - \theta_2)\sin\phi_1\sin(\phi_1 - \phi_2) \\ &\equiv E\cos T + F\sin T \end{aligned}$$

Manuscript received April 21, 1966.

[1] W. P. Ayres, "Broad band quarter-wave plates," *IRE Trans. on Microwave Theory and Techniques*, vol. MTT-5, pp. 258–261, October 1957.
[2] P. J. Meier, "Wide band polarizer in circular waveguide loaded with dielectric discs," *IEEE Trans. on Microwave Theory and Techniques*, vol. MTT-13, pp. 763–767, November 1965.
[3] A. J. Simmons, "A compact broad-band microwave quarter-wave plate," *Proc. IRE*, vol. 40, pp. 1089–1090, September 1952.

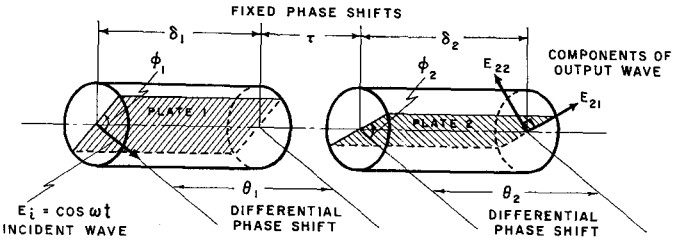

Fig. 1. Two plate polarizer schematic.

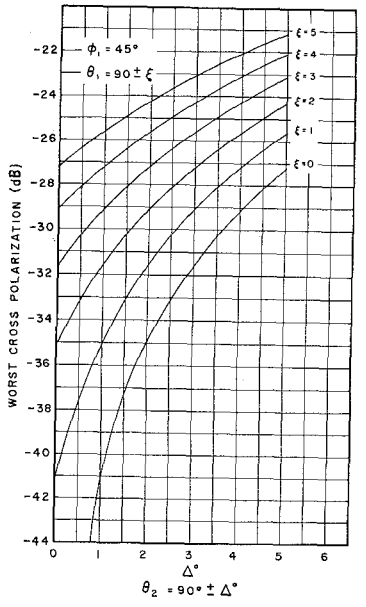

Fig. 2. Worst cross polarization for $\phi_1 = 45$.

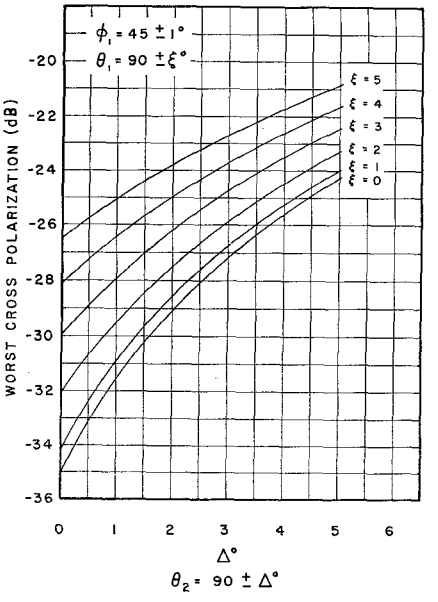

Fig. 3. Worst cross polarization for $\phi_1 = 45 \pm 1$.

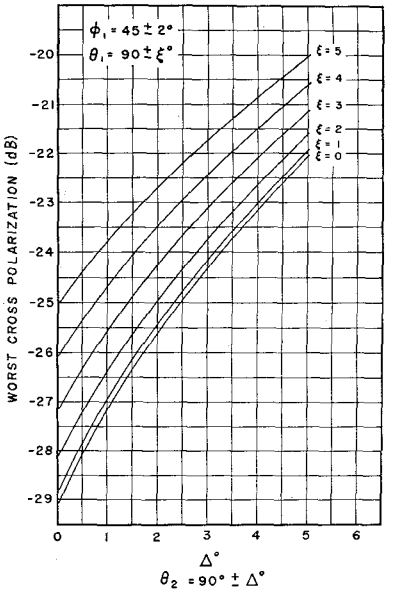

Fig. 4. Worst cross polarization for $\phi_1 = 45 \pm 2$.

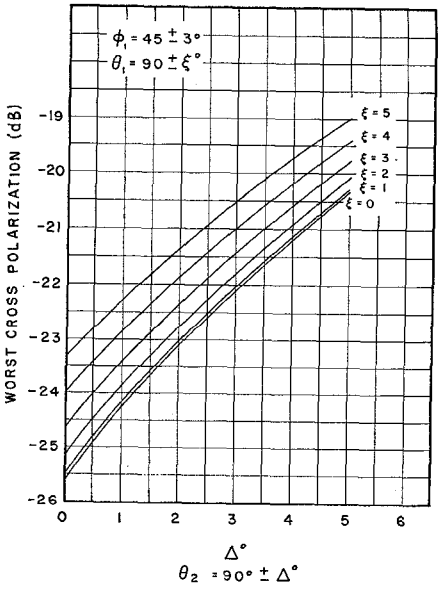

Fig. 5. Worst cross polarization for $\phi_1 = 45 \pm 3$.

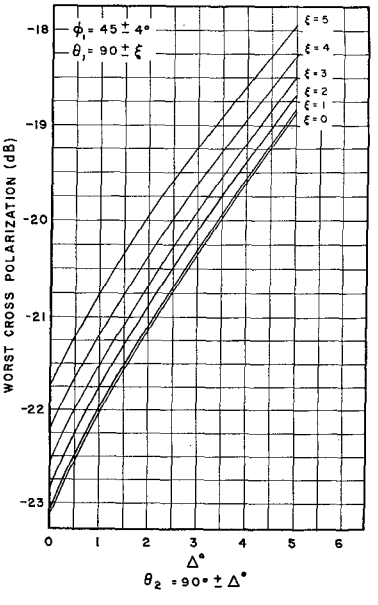

Fig. 6. Worst cross polarization for $\phi_1 = 45 \pm 4$.

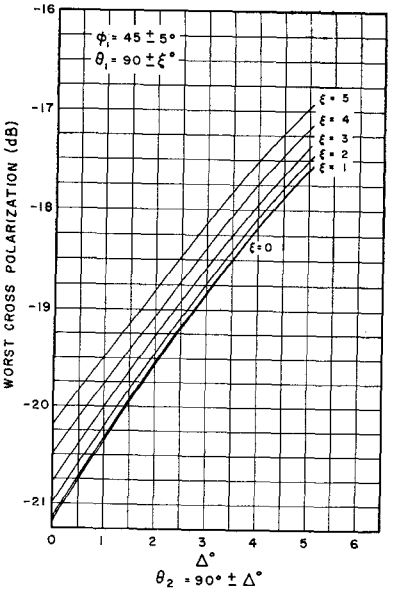

Fig. 7. Worst cross polarization for $\phi_1 = 45 \pm 5$.

$$E_{22} = \cos(T - \theta_1)\cos\phi_1 \sin(\phi_1 - \phi_2) - \cos T \sin\phi_1 \cos(\phi_1 - \phi_2) \equiv C\cos T + D\sin T \quad (1)$$

where

$$T = \omega t - \delta_1 - \delta_2 - \tau \quad (2)$$

and C, D, E, F are defined by these equations.

The resultant of these two components sweeps out an ellipse as T increases, and the cross polarization is simply the ratio of the semi-major and semi-minor axes. These may be found by rotating the E_{21}, $E_{22}(X, Y)$ axes by a positive angle α to a new pair of axes (x, y). α is chosen so that the cross product xy of the ellipse equation in (x, y) coordinates vanishes.

This criterion is found to be

$$\alpha = \frac{1}{2}\tan^{-1}\left\{\frac{2(CE + DF)}{E^2 + F^2 - C^2 - D^2}\right\} \quad (3)$$

and the ellipse equation is then

$$\frac{x^2}{R^2} + \frac{y^2}{S^2} = 1 \quad (4)$$

where

$$R^2 = \left[\frac{(CF - DE)^2}{(C^2 + D^2)\cos^2\alpha - (CE + DF)\sin 2\alpha + (E^2 + F^2)\sin^2\alpha}\right] \quad (5)$$

and

$$S^2 = \left[\frac{(CF - DE)^2}{(C^2 + D^2)\sin^2\alpha + (CE + DF)\sin 2\alpha + (E^2 + F^2)\cos^2\alpha}\right].$$

The cross polarization is then

$$\text{C.P.}_{\text{db}} = -10\left|\log\left(\frac{R^2}{S^2}\right)\right|. \quad (6)$$

The necessary functions of C, D, E, F are found to be

$$\begin{aligned} C^2 + D^2 &= \cos^2\phi_1 \cdot \sin^2(\phi_1 - \phi_2) + \sin^2\phi_1 \cdot \cos^2(\phi_1 - \phi_2) - \tfrac{1}{2}\cdot\sin 2\phi_1 \cdot \sin(2\phi_1 - 2\phi_2)\cdot\cos\theta_1 \\ E^2 + F^2 &= \cos^2\phi_1 \cdot \cos^2(\phi_1 - \phi_2) + \sin^2\phi_1 \cdot \sin^2(\phi_1 - \phi_2) + \tfrac{1}{2}\cdot\sin 2\phi_1 \cdot \sin(2\phi_1 - 2\phi_2)\cdot\cos\theta_1 \\ CE + DF &= \tfrac{1}{2}\cdot\cos 2\phi_1 \cdot \sin(2\phi_1 - 2\phi_2)\cdot\cos\theta_2 + \tfrac{1}{2}\sin^2(\phi_1 - \phi_2)\cdot\sin 2\phi_1 \cdot\cos(\theta_1 - \theta_2) - \tfrac{1}{2}\cos^2(\phi_1 - \phi_2) \cdot\sin 2\phi_1 \cdot\cos(\theta_1 + \theta_2). \end{aligned} \quad (7)$$

Figures 2 to 7 give computed results for the worst cross polarization (ϕ_2 was varied in steps and worst value chosen) for various reasonable combinations of $\phi_1, \theta_1, \theta_2$. The expression for cross polarization may be greatly simplified by assuming differential phase shifts close to $\pi/2$ and ϕ_1 close to $\pi/4$, if desired.

ACKNOWLEDGMENT

The author is indebted to W. Lavrench for a discussion of this work.

R. W. BREITHAUPT
Radio and Elect. Engrg. Div.
National Research Council
Ottawa, Canada

Solid-State Plasma Controlled Nonreciprocal Microwave Device

Various types of nonreciprocal microwave devices have been developed through the use of the tensor permeability of magnetic materials such as ferrites.[1] In a solid-state plasma such as a semiconductor, the conductivity becomes a tensor quantity under a dc magnetic field. Toda[2] developed an isolator using a solid-state plasma under a transverse magnetic field and obtained the isolation ratio of about 10 dB. Recently, we have reported the result of the experimental observation of the microwave Faraday effect in a solid-state plasma waveguide under a longitudinal magnetic field.[3] It was found that a large amount of rotation of the plane of polarization with very small attenuation of power can be obtained in a solid-state plasma under a relatively high magnetic field. In this paper, an experimental nonreciprocal microwave device which makes use of the Faraday rotation in a solid-state plasma is presented.

The experimental microwave device consists of two rectangular waveguides, two resistance vanes, and a solid-state plasma Faraday rotator as shown in Fig. 1. The Faraday rotator consists of a circular waveguide (7 mm ID) in which a disk (7 mm $D \times 1$ mm T) of an n-type InSb single crystal ($n_e = 10^{14}/\text{cm}^3$, $\mu_e = 70\,000$ cm^2/V.s, $\rho = 0.1$ Ω-cm, at 77°K) and two quarter-wavelength impedance transformers ($\epsilon_r = 4$) are mounted as shown in Fig. 1. The impedance transformers are placed at both sides of the InSb disk to minimize the wave reflections from the surfaces of the InSb disk. The resistance vanes are mounted in such a way as to attenuate the components of electric field which are parallel to the broad walls of the rectangular guides. The transitions between the rectangular and circular guides are made smooth by means of tapered transitions. The two rectangular guides are rotated 45° with respect to each other.

A linearly polarized wave, after passing through the solid-state plasma, becomes an elliptically polarized wave in which the major axis of polarization is rotated through an angle with respect to the plane of polarization of the incident wave. The angle of the Faraday rotation Θ and the ellipticity of polarization $\mathcal{E}$ vary as a function of the magnetic field B_0. (Details of the principle of the Faraday effect in a solid-state plasma can be found elsewhere.[3]) The direction of the rotation depends on the direction of propagation with respect to the direction of the magnetic field. For example, if the magnetic field is applied in the direction as shown in Fig. 1, the wave propagating from left to right experiences clockwise rotation due to the Faraday rotator, while the wave propagating in the opposite direction experiences counterclockwise rotation.

Let T be the transmission coefficient of the Faraday rotator. Then the insertion loss of the device for the transmission from left to right will be

$$L_1 = -10\log\left[T^2\{\cos^2(\Theta - 45°) + \mathcal{E}^2\sin^2(\Theta - 45°)\}\right]$$

and for the transmission in the opposite direction, we get

$$L_2 = -10\log\left[T^2\{\cos^2(\Theta + 45°) + \mathcal{E}^2\sin^2(\Theta + 45°)\}\right]$$

Thus we can achieve nonreciprocal transmission through this device. By varying the magnetic field, we can control Θ and in turn we can control L_1 and L_2. When $\Theta = 45° + n \times 180°$ where n is an integer, the difference between L_1 and L_2 will be maximized. By reversing the direction of the magnetic field, we can switch L_1 and L_2 from maximum to minimum or vice versa. Thus the experimental device can be used as an attenuator, isolator, or switch.

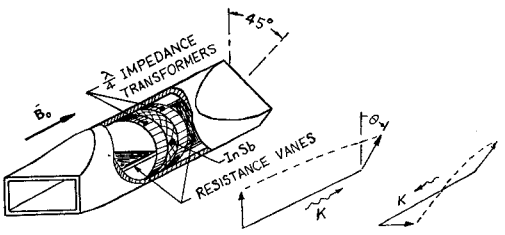

Fig. 1. An experimental solid-state plasma controlled nonreciprocal microwave device.

Manuscript received August 23, 1966. This work is partly based on dissertation research by the author and is supported in part by a NASA research grant.

[1] See, for example, C. L. Hogan, "The elements of nonreciprocal microwave device," *Proc. IRE*, vol. 44, pp. 1345–1368, October 1956; and B. Lax and K. J. Button, *Microwave Ferrites and Ferrimagnetics*. New York: McGraw-Hill, 1962, ch. 12.

[2] M. Toda, "A new isolator using a solid-state plasma waveguide," *IEEE Trans. on Microwave Theory and Techniques (Correspondence)*, vol. MTT-12, pp. 126–127, January 1965.

[3] H. J. Kuno and W. D. Hershberger, "Observation of microwave Faraday rotation in a solid-state plasma," *Proc. IEEE (Letters)*, vol. 54, pp. 978–979, July 1966.

The characteristics of the experimental device were measured under various magnetic fields using the set-up as shown in Fig. 2. The device was placed between a pair of poles of a magnet and immersed in liquid nitrogen to cool the InSb crystal so that μ_e and ρ were increased. The klystron was tuned to $f = 35.95$ GHz. Figure 3 shows the measured nonreciprocal transmission characteristics. The points where $B_0 = 1.1$, 2.8, and 8.5 kg correspond to $\Theta = 225°$, 135°, and 45°, respectively. In particular, at $B_0 = 8.5$ kg, an excel-